MIT Libraries | DSpace@MIT

MIT Open Access Articles

On the oscillatory nature of heat transfer in steady annular flow

The MIT Faculty has made this article openly available. ***Please share*** how this access benefits you. Your story matters.

Citation: Su, Guan-Yu et al. "On the oscillatory nature of heat transfer in steady annular flow." International Communications in Heat and Mass Transfer 108 (November 2019): 104328 © 2019 Elsevier Ltd

As Published: http://dx.doi.org/10.1016/j.icheatmasstransfer.2019.104328

Publisher: Elsevier BV

Persistent URL: https://hdl.handle.net/1721.1/126766

Version: Author's final manuscript: final author's manuscript post peer review, without publisher's formatting or copy editing

Terms of use: Creative Commons Attribution-NonCommercial-NoDerivs License

Massachusetts Institute of Technology

On the oscillatory nature of heat transfer in steady annular flow

Guan-Yu Su[a,*], Francesco Paolo D'Aleo[b], Bren Phillips[a], Robin Mark Streich[b], Eissa Al-Safran[c], Jacopo Buongiorno[a], Horst-Michael Prasser[b]

[a]*Department of Nuclear Science and Engineering, Massachusetts Institute of Technology (MIT), Cambridge, Massachusetts 02139, USA*
[b]*Labor für Kernenergiesysteme, Institut für Energietechnik, ETH Zürich, 8092 Zürich, Switzerland*
[c]*Department of Petroleum Engineering, Kuwait University, Kuwait City, Kuwait*

ABSTRACT

Using a combination of high-speed infrared thermography and electrical-conductance sensors, we observe the surprisingly large effect of surface waves on the instantaneous heat transfer response at the heated wall in nominally-steady upward annular flow of steam-water mixtures. While the heat flux applied at the wall is constant, the passage of the waves causes significant periodic oscillations of the local heat transfer coefficient and wall superheat in the forced convective evaporation regime, with amplitudes and periods much higher than the fluctuations due to turbulent eddies. We discuss the physical mechanisms potentially responsible for the experimental observations.

KEYWORDS

Diabatic Annular Flow, Heat Transfer Oscillation, Waves, Liquid Film Sensor, IR Thermography

1. Introduction

Two-phase flow and heat transfer are transport phenomena encountered in diverse industrial applications ranging from power systems to refineries, from food factories to oil wells, from chemical plants to refrigeration systems. A rich set of hydrodynamic and thermal instabilities may occur in two-phase flows: density-wave oscillations, Ledinegg instability, Rayleigh-Taylor and Kelvin-Helmotz interfacial instabilities, flow pattern transition instability, geysering, water hammering and the infamous boiling crisis or critical heat flux, all of which have the potential to cause large, uncontrolled excursions of the thermal and hydraulic parameters. A comprehensive review of these instabilities is provided in [1,2]. The common understanding is that clever design and prudent operations can suppress or eliminate such instabilities, and thus two-phase flow will exhibit a benign behavior with steady values of the important engineering quantities, e.g., pressure drop, flow rate, and heat transfer coefficient (HTC).

Here we show that this is not necessarily true in the case of stable annular flow of steam-water mixtures in diabatic channels. In such situation, there exists a continuous liquid film slowly moving along the wall and a fast-moving steam core (sometimes laden with small droplets) occupying the center of the channel. Heat transfer from the wall occurs via convection within the liquid film and by evaporation at the liquid film surface. No bubble nucleation normally occurs in the film. The resulting heat transfer regime is known

*Corresponding author.
E-mail address: gysu@mit.edu

as forced convective evaporation, and is present, for example, in the tubes of fossil fuel boilers and the fuel assemblies of boiling-water nuclear reactors. The wavy nature of the liquid film in annular flow is well understood: rapid changes in film thickness can be caused by large disturbance waves, smaller ripple waves or even wisps of liquid bridging the channel [3]. However, the effect of such changes on forced convective evaporation heat transfer has long been ignored or thought to be negligible. This is somewhat understandable: the vast majority of studies on the dynamics of the liquid film in annular flow are conducted in adiabatic air-water systems [4-6], while measurements of forced convective evaporation heat transfer typically use thermocouples or resistive temperature detectors, lacking the spatial and temporal resolutions necessary to detect wall temperature oscillations associated with the waves [7,8]. It follows that the heat transfer coefficient correlations for forced convective evaporation commonly recommended in textbooks and literature [2, 9-11] can be used only to predict time-averaged quantities.

In this study, we address these shortcomings by using a modern multi-physics diagnostics combining synchronized infrared (IR) thermography and electrical conductance-based liquid film thickness sensors (LFS), integrated within a two-phase flow loop. Since such diagnostics provides the instantaneous 2D wall superheat, 2D HTC and quasi-2D liquid film thickness, we are able to detect large-scale periodic oscillations of the local wall superheat and HTC induced by waves at nominally steady-state annular flow.

2. Experimental setup and diagnostics

The experimental apparatus is shown in Fig. 1 (a). A specially-designed heater with an Indium-Tin-Oxide (ITO) Joule-heated layer (~700 nm thickness, 9 mm × 94.5 mm area), deposited on a sapphire substrate of 1 mm thickness (see Fig. 1 (c)) is integrated into the test section having 1 cm × 1 cm square cross section and 190.6 mm length (see Fig. 1 (b)). Using a high-speed IR camera, we measure the temperature distribution on the surface of the heater with a spatial resolution of 100 μm at a frame rate of 2 kHz. Extracting the temperature distribution and heat flux to water from the IR signal requires a fairly complex calibration procedure that accounts for the conjugate radiative and conductive heat transfer within the heater. Details are reported in reference [12].

The liquid film thickness is measured by a LFS, either installed separately downstream of the IR heater (Fig. 1 (d)) or integrated onto the IR heater (Fig. 1 (e)). We use the separate LFS at all the test conditions, while implement the (much more delicate) integrated LFS at a single selected condition to validate the results of the separate sensors. Such LFS provides measurements at 8 longitudinal locations and 8 transversal locations. The sampling frequency for this sensor is 10 kHz, with a precision of 2.5 μm and an overall uncertainty of 13 μm on the measured thickness of the film. A small amount of KNO_3 is added prior to each test, to obtain an aqueous solution with conductivity ~200 $\mu S \cdot cm^{-2}$, which enables accurate measurement by the LFS. All the thermo-physical properties of the solution are essentially identical to deionized water; we also verify that neither KNO_3 deposition nor other scale formations occur on the heat transfer surface during the experiments.

The test section is incorporated in a flow loop capable of generating upward annular flow of steam and water mixtures with carefully-controlled values of the governing parameters within the following ranges: mass flux G from 700 to 1400 $kg \cdot m^{-2} \cdot s^{-1}$, and steam quality x from 0.01 to 0.08, for a total of 11 tests. At each test, the imposed planar heat generation rate at the wall q'' can vary from 0 to 2000 $kW \cdot m^{-2}$. The tests are conducted at conditions for which bubble nucleation in the liquid film does not occur. The system

pressure is slightly above atmospheric for all tests. The supplemental material contains additional details on the experimental apparatus and instrumentation setup.

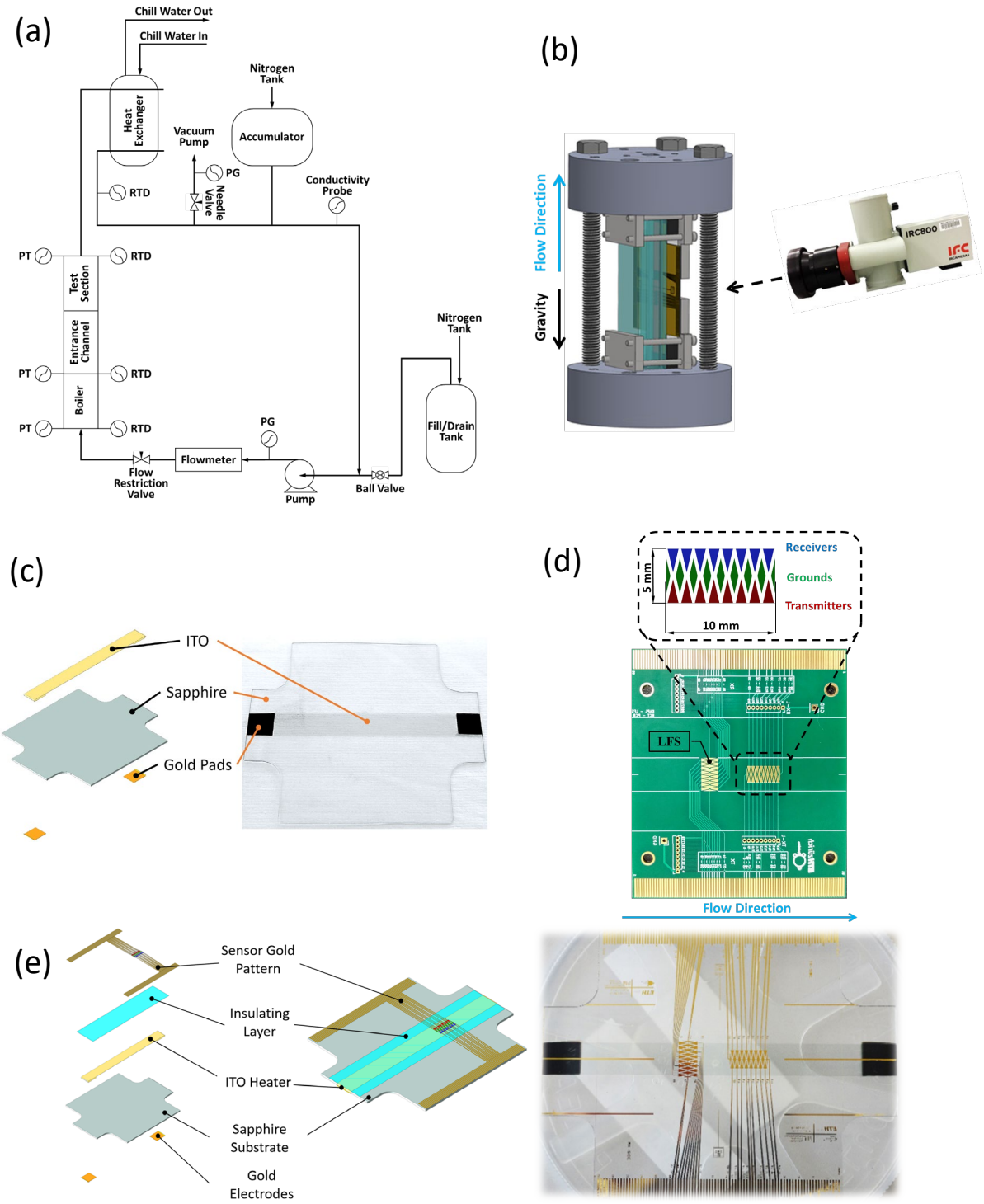

Fig. 1. Experimental Apparatus: (a) schematic of the flow loop; (b) test section with the high speed IR camera setup; (c) configuration of the IR heater; (d) configuration of the separate LFS; (e) configuration of the integrated LFS.

3. Results and discussion

3.1. Separate IR heater and LFS

Fig. 2 shows (a) typical time histories for the measured wall superheat (averaged over a transversal chord on the heater), (b) the heat flux to water (averaged over the same transversal chord), and (c) the corresponding heat transfer coefficient (defined as the ratio of heat flux to water to the wall superheat). Note that the large-amplitude oscillations of the temperature, the heat flux to water and the heat transfer coefficient, are well beyond the measurement uncertainties, i.e., 0.49 °C for the surface temperature, 1.7% for the heat flux to water and 6% for the heat transfer coefficient. Such oscillations are not due to a two-phase flow instability, i.e., the pressure drop and mass flux throughout the loop are steady, and the imposed planar heat generation rate is constant. These large oscillations are also not due to turbulent eddies in the liquid film, for which we estimate the maximum turbulent temperature fluctuations using the mixing length model for turbulence [2,13]. The estimated temperature fluctuations induced by turbulence is of the order of 1 °C in the test condition shown in Fig. 2, occurring on a time scale that is much shorter than the period observed. More detailed information on the turbulent temperature fluctuation estimate is in the supplemental material.

In Fig. 2 (d), the plot shows the oscillations of the liquid film thickness due to surface waves measured with a separate LFS at a location 193.6 mm downstream of the IR heater. Such film thickness oscillations are expected in annular flow [3]. There is a time shift between the temperature reading and the film thickness reading, because they are not co-located spatially. The shift is calculated from the cross-correlation of the two readings, c_{12}:

$$c_{12}(\tau) = \frac{1}{\Delta t}\int_{t_1}^{t_1+\Delta t} [y_1(t) - \bar{y}_1][y_2(t+\tau) - \bar{y}_2]dt \tag{1}$$

where Δt is the time interval of interest, τ is the time shift, $y_1(t)$ and $y_2(t)$ are two univariate time series, $\bar{y}_1$ and $\bar{y}_2$ are their means, respectively. The resulted time shift for the film thickness signal in Fig. 2 (d) is about 0.0595 s. The transit velocity calculated from this time shift is 3.25 m·s^{-1}, which is within the range 4.56 ± 2.24 m·s^{-1} typically measured for liquid film waves at such flow conditions [14, 15]. Similar results are obtained for all tests conducted. Therefore, we surmise that the temperature oscillations are due to the passage of the waves, i.e., the crests of the liquid film thickness appear to coincide with the crests of the temperature and the troughs of the heat flux and HTC.

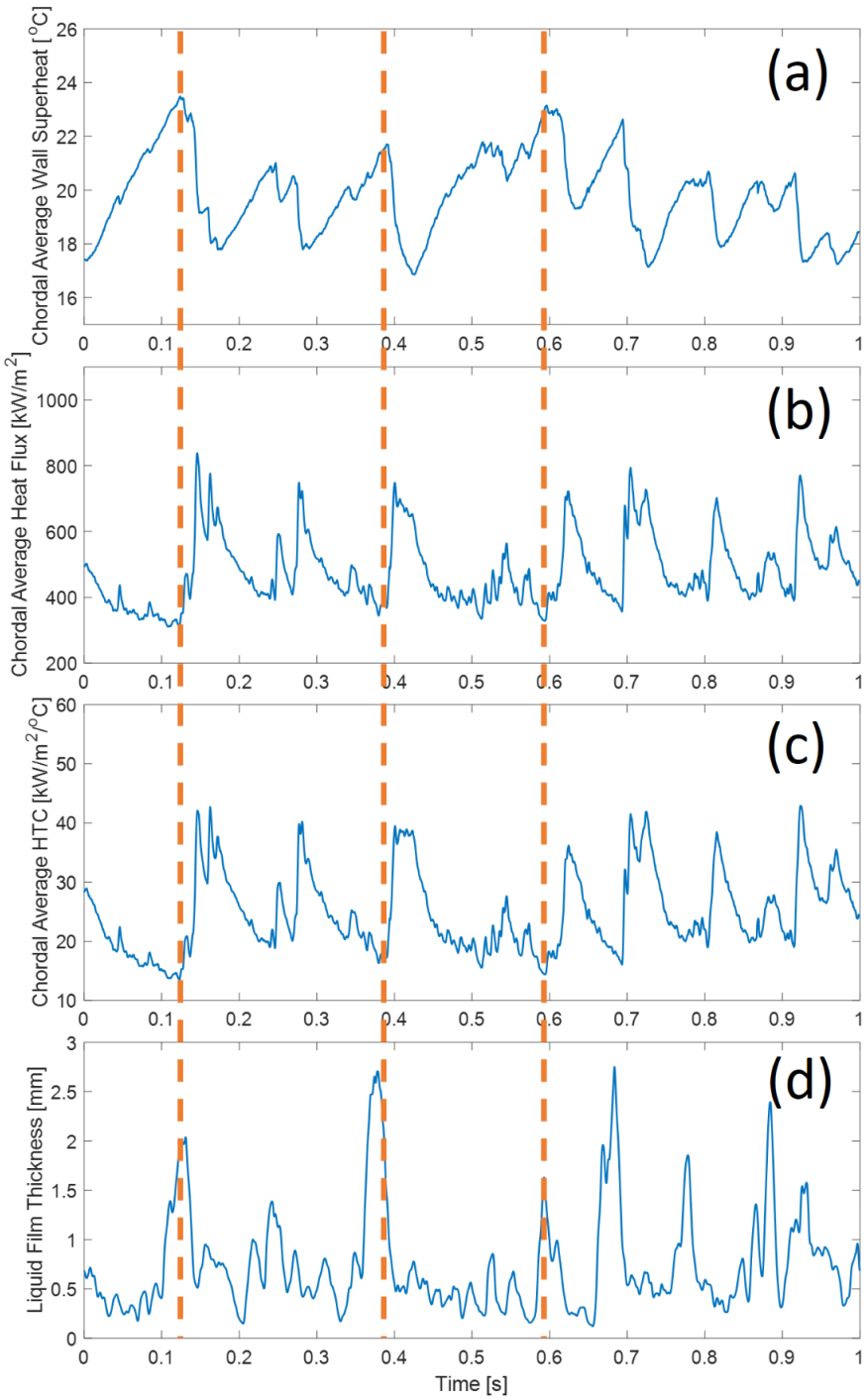

Fig. 2. Time history of (a) the chordal average wall superheat, (b) the chordal average heat flux to water, (c) the chordal average heat transfer coefficient, and (d) the liquid film thickness. The dashed lines show that peaks of the wall superheat correspond to minima of the heat flux to water and the heat transfer coefficient. This test is for G = 1050 kg·m^{-2}·s^{-1}, x_e = 0.016, and planar heat generation rate q'' = 493 kW·m^{-2}.

Due to the non-co-located test setup, the aforementioned interpretation of the heat transfer oscillations may be questionable. The above interpretation would be accurate under two assumptions: first, the film characteristics do not change as the film travels from the location of IR camera to the location of the LFS;

second, the film and wave velocities are known and constant. To remove the ambiguity in the interpretation of the heat transfer data, we conduct a test with a co-located IR heater and LFS, as explained next.

3.2. Integrated IR heater and LFS

The integrated IR heater and LFS is shown in Fig. 1 (e). It allows obtaining first-of-kind heat transfer and liquid film data in annular flow that are both synchronized (within ±250 μs) and co-located (within ±625 μm). In Fig. 3, the temperature and HTC signals and the liquid film thickness signal at q''= 341.3 kW/m^2 are superimposed for ease of interpretation, where the measured quantities are from the same location. It can be seen that the temperature peaks correlate very well with the liquid film thickness peaks. The highest HTC occurs immediately after the passage of a wave, while the lowest HTC occurs at the peak of the liquid film thickness. In addition, the HTC gradually decreases until the passage of the following large wave, which leads to a slow recovery of the wall temperature. Such dynamic process is identical to our observation for the tests with the separate LFS set-up shown in Fig. 2, which gives confidence in the separate IR and LFS measurements.

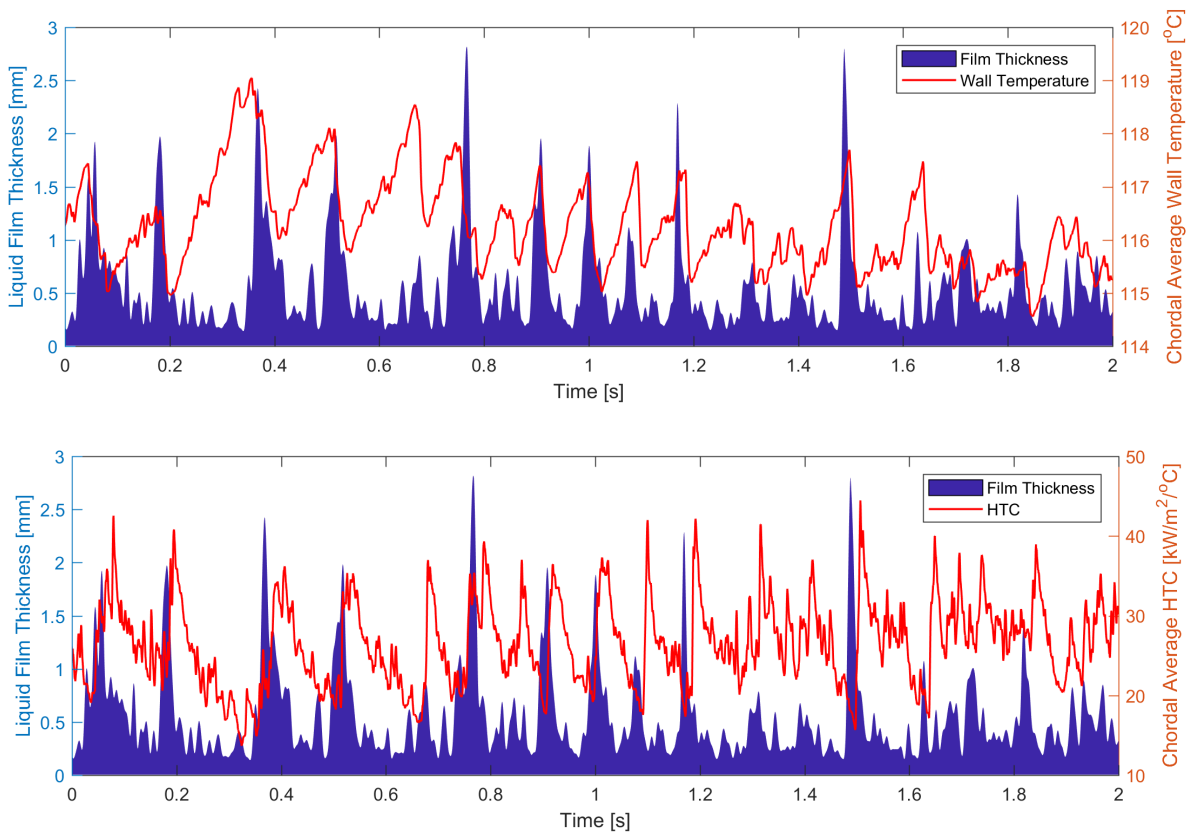

Fig. 3. Comparison of temperature and htc with liquid film thickness at a specific longitudinal LFS location. This test is for G = 1050 kg·m^{-2}·s^{-1}, x_e = 0.016, and planar heat generation rate q''= 341.3 kW/m^2.

3.3. Mechanism and model

We hypothesize that the local liquid film mass flow rate also oscillates in unison with the oscillations of the liquid film thickness, according to the so-called triangular relationship of liquid film thickness, liquid film mass flow rate and local pressure gradient [3]. When a wave crest approaches, the liquid velocity in the flow direction decreases due to the sharp rise in liquid film thickness, which results in impaired heat

transfer, high wall superheat, and low HTC. Conversely, when a wave crest departs and a trough is present, the liquid velocity increases due to the sharp drop of the film thickness. In such condition, heat transfer is promoted and thus wall superheat reaches a minimum value, which in turn maximizes the HTC. This acceleration effect diminishes before the following wave crest approaches, which results in a gradual decrease of heat transfer and slow recovery of the wall superheat. In addition, the HTC signal exhibits a time delay with respect to the film thickness signal, likely due to the postulated local mass flow rate oscillation.

To examine the plausibility of our hypothesis, we develop a one-dimensional model that simulates the time-dependent fluid flow and conjugate heat transfer within the film and the heater, including the effect of the waves. The momentum and energy conservation equations assume the following forms.

In the liquid film:

$$\left[\varepsilon_M(y_l) + \frac{\mu_l}{\rho_l}\right]\frac{\partial v}{\partial y_l} = \tau_w\left[1 - \frac{y_l}{\delta(t)}\right] + \tau_i\frac{y_l}{\delta(t)} \tag{2}$$

$$\frac{\partial T_l}{\partial t} = \frac{\partial}{\partial y_l}\left\{[\varepsilon_H(y_l) + \alpha_l]\frac{\partial T_l}{\partial y_l}\right\} \tag{3}$$

In the heater:

$$\frac{\partial T_s}{\partial t} = \alpha_s\frac{\partial^2 T_s}{\partial y_s^2} \tag{4}$$

where y is the coordinate perpendicular to the wall, t is time, δ is the instantaneous thickness of the film, v is velocity within the liquid film, T is temperature, μ is viscosity, ρ is density, τ is shear stress, α is thermal diffusivity, ε_M and ε_H are the turbulent momentum and heat diffusivities, respectively; the subscripts l, s, w and i stand for liquid, solid (heater), wall, and steam-water interface, respectively. More information is in the supplemental material.

Since the local instantaneous liquid film mass flow rate is not measured in this work, we postulate that it follows the history of the film thickness signal, while conserving the time-averaged value, which of course is measured. In addition, the model takes the measured instantaneous film thickness from the integrated LFS as input and solves the equations to get the instantaneous velocity and temperature distributions within the liquid film and the heater. We found that a 15 ms time delay of the mass flow rate with respect to the film thickness gives the best agreement with the measured wall temperature and HTC in average value, oscillating amplitude, frequency, phase and shape, as shown in Fig. 4. Such agreement lends credence to the postulation of an out-of-phase liquid mass flow rate oscillation.

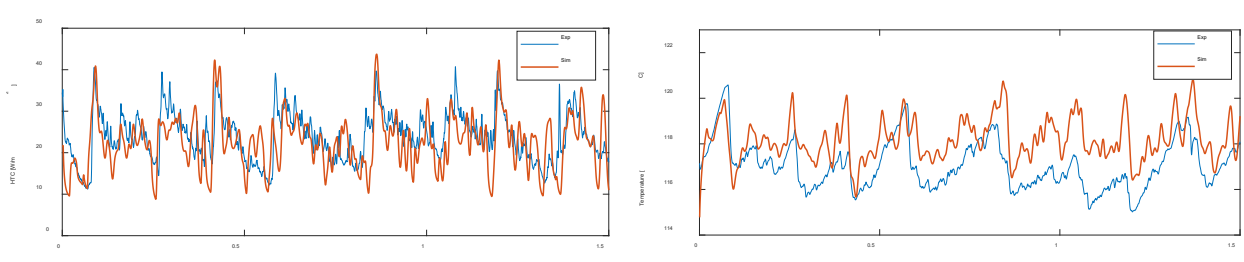

Fig. 4. Comparison of heated wall HTC and temperature between experiment (Exp) and simulation (Sim) at G = 1050 kg·m^{-2}·s^{-1}, x_e = 0.016, and planar heat generation rate q''= 341.3 kW/m^2.

4. Conclusions

In conclusion, our experiments suggest that the passage of liquid film waves in steady-state upward annular flow of a steam and water two-phase mixture produces large, and hitherto undetected, oscillations of the local heat transfer on the heated wall. We hypothesize that the combined effect of thickness and mass flow rate oscillations of the liquid film leads to the heat transfer oscillations in the forced convective evaporation regime. Direct measurement of the velocity field in the liquid film, e.g., by particle image velocimetry (PIV), would be required to conclusively confirm our hypothesis. Such large wall temperature oscillations (> 5°C) and the accompanying liquid film mass flow rate oscillations may induce thermal fatigue and potentially trigger early local dry-out at higher heat flux, which often lead to system failure in industrial applications such as coal-fired boiler tubes or nuclear reactor fuel assemblies.

Acknowledgement

The authors gratefully acknowledge the financial support of the Knolls Atomic Power Laboratory (KAPL). The authors acknowledge Dr. Lin-Wen Hu from the MIT Nuclear Reactor Lab (NRL) for sharing some equipment used in the present study. The authors are also thankful to Mr. Robers Lukas from ETH Zurich for the good discussion on the experimental results.

References

[1] L. S. Tong and Y. S. Tang, Boiling Heat Transfer and Two-Phase Flow (2 ed). Taylor&Francis Press (1997).

[2] N. E. Todreas and M. S. Kazimi, Nuclear Systems-Volume 1, Taylor&Francis (2012).

[3] G. F. Hewitt, Annular Two-Phase Flow (1 ed), Pergamon Press (1970).

[4] N. S. Hall-Taylor, G. F. Hewitt and P.M.C. Lacey, The motion and frequency of large disturbance waves in annular two-phase flow of air-water mixtures, Chem. Eng. Sci. 18 (1963) 537-552.

[5] P. Sawant, M. Ishii, T. Hazuku, T. Takamasa, and M. Mori, Properties of Disturbance Waves in Vertical Annular Two-Phase Flow, Nucl. Eng. Des. 238 (2008) 3528-3541.

[6] Y. Zhao, C. N. Markides, O. K. Matar, and G. F. Hewitt., Disturbance Wave Development in Two-Phase Gas-Liquid Upwards Vertical Annular Flow, Int. J. Multiphase Flow 55 (2013) 111-129.

[7] D. L. Bennett, and J. C. Chen, Forced convective boiling in vertical tubes for saturated pure components and binary mixtures, AICHE J. 26 (1980) 454-461.

[8] J. R. Barbosa, G. F. Hewitt, and S. M. Richardson, Forced Convective Boiling of Steam–Water in A Vertical Annulus at High Qualities, Exp. Therm. Fluid Sci. 26 (2002) 65-75.

[9] J. C. Chen, Correlation for boiling heat transfer to saturated fluids in convective flow, Ind. Eng. Chem. Process Des. Dev. 5 (1966) 322-329.

[10] S. G. Kandlikar, A General Correlation for Saturated Two-Phase Flow Boiling Heat Transfer inside Horizontal and Vertical Tubes, J. Heat Transfer 112 (1990) 219-228.

[11] V. V. Klimenko, A Generalized Correlation for Two-Phase Forced Flow Heat Transfer, Int. J. Heat Mass Transfer 31 (1988) 541-552.

[12] M. Bucci, A. Richenderfer, G-Y. Su, T. McKrell, and J. Buongiorno, Int. J. Multiphase Flow **83**, 115 (2016).
[13] S. B. Pope, Turbulent Flows (1 ed). Cambridge University Press (2000).
[14] G-Y. Su, Thermohydraulics and Suppression of Nucleate Boiling in Upward Two-Phase Annular Flow: Probing Multiscale Physics by Innovative Diagnostics, Ph.D. Dissertation, MIT (2018).
[15] P. B. Whalley, Boiling Condensation and Gas-Liquid Flow, Clarendon Press (1990).